Tension-Induced Morphological Transition in Mixed Lipid Bilayers

S. Komura* and N. Shimokawa

Department of Chemistry, Faculty of Science, Tokyo Metropolitan University, Tokyo 192-0397, Japan

D. Andelman

School of Physics and Astronomy, Raymond and Beverly Sackler Faculty of Exact Sciences, Tel Aviv University, Ramat Aviv 69978, Tel Aviv, Israel

Recently, Rozovsky et al. reported on the morphology and dynamics of superstructures in three-component lipid bilayers containing saturated lipid, unsaturated lipid, and cholesterol (Rozovsky, S.; Kaizuka, Y.; Groves, J. T. *J. Am. Chem. Soc.* **2005**, *127*, 36). We suggest that the observed sequence of the striped-to-hexagonal morphological transition in mixed bilayers can be attributed to an enhanced membrane surface tension that is induced by the vesicle adhesion onto the solid surface.

I. Introduction

Raft domains in biological cell membranes are associated with membrane signaling pathways and have attracted a great deal of interest in recent years.[1,2] Because of the complexity of biological membranes, a minimal model to investigate rafts (or more precisely, domain formation) consists of three-component lipid bilayers containing saturated and unsaturated lipids as well as cholesterol. These three-component systems have been investigated both at the air−water interface and in artificial vesicles.[3−5] Complex phase separation and the appearance of domains have been observed using fluorescence techniques. Such a phase separation occurs between a liquid-disordered phase rich in unsaturated lipid (e.g., DOPC) and a liquid-ordered phase rich in saturated lipid (e.g., sphingomyelin) and cholesterol.[3−5]

Recently, Rozovsky et al.[6] reported on the morphology and dynamics of *superstructures* in a ternary mixture of sphingomyelin, DOPC, and cholesterol. A giant $10 \, \mu m$ unilamellar vesicle is placed in contact with a lipid bilayer that is supported on top of a silica surface. The experimental setup is shown schematically in Figure 1. Fluorescence microscopy is used to monitor the creation and temporal evolution of domains on the adhering vesicle. The bound vesicle exhibits a gradual pattern transformation under the adhesion constraints. In a number of cases, the nonadhering top region of the vesicle, which can be directly imaged by the microscope, first exhibits a striped pattern of well-characterized stripe width. As time evolves, the striped pattern transforms quite abruptly into another pattern consisting of an ordered hexagonal lattice of circular domains, as is schematically represented in Figure 1. The transformation of the stripes into circular domains is seen first as a "pinch-off" instability of the stripe tip. In a matter of a few seconds, the entire striped pattern is replaced by circular domains having roughly the same diameter as the original stripe width. As time progresses even further, the hexagonal pattern of circular domains becomes less
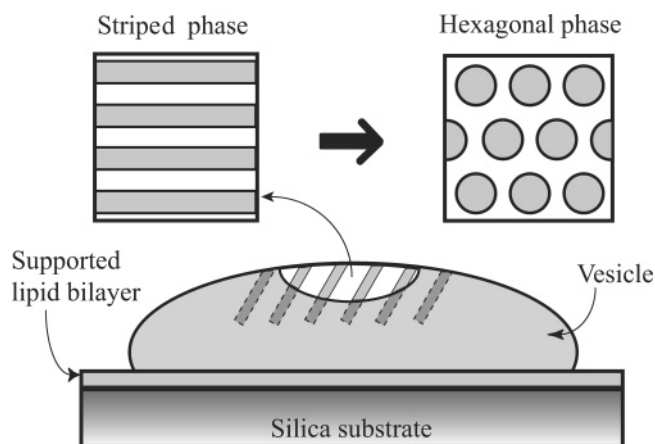
Figure 1. Schematic representation of a mixed vesicle adhering onto a supported lipid bilayer. The nonadhering upper region of the vesicle exhibits a morphological transition from a striped phase to a hexagonal phase with the elapse of time. The size of the vesicle is on the order of $10 \, \mu m$, and the period of the modulation is roughly $1 \, \mu m$. Details of the experiment are described in ref 6.

ordered. Because of the large size of the vesicle, its upper part shown in Figure 1 of ref 6 is a few micrometers above the supported lipid bilayer and is not in contact with the silica surface. The shape of the vesicle and its contact area change as the pattern evolves. Note that the field of view is adjusted to capture the shape evolution.

It is known that surface tension can induce the adhesion of a vesicle onto a substrate or to another vesicle,[7] the reason being that the membrane surface tension suppresses thermal fluctuations and promotes its adhesive properties. A self-consistent treatment of such a problem predicted the conditions for tension-induced adhesion.[7] On the other hand, it was reported that the spreading of red blood cells on a substrate produces finite surface tension that can even cause them to rupture.[8] More recent experiments on the pulling of nanotubes from adhered vesicles revealed that membrane tension strongly increases during the pulling and elongation of nanotubes.[9]

* Corresponding author. E-mail: komura@comp.metro-u.ac.jp.

(1) Simons, K.; Ikonen, E. *Nature* **1997**, *387*, 569.
(2) Brown, D. A.; London, E. *J. Biol. Chem.* **2000**, *275*, 17221.
(3) Veatch, S. L.; Keller, S. L. *Phys. Rev. Lett.* **2002**, *89*, 268101.
(4) Baumgart, T.; Hess, S. T.; Webb, W. W. *Nature* **2003**, *425*, 821.
(5) Veatch, S. L.; Keller, S. L. *Phys. Rev. Lett.* **2005**, *94*, 148101.
(6) Rozovsky, S.; Kaizuka, Y.; Groves, J. T. *J. Am. Chem. Soc.* **2005**, *127*, 36.

(7) Seifert, U. *Phys. Rev. Lett.* **1995**, *74*, 5060.
(8) Hategan, A.; Law, R.; Kahn, S.; Discher, D. E. *Biophys. J.* **2003**, *85*, 2746.

In view of these works, we explore the relation between an increase in surface tension and lateral morphological transitions that can occur on the membrane plane. The aim of this paper is to point out that the observed sequence of the striped-to-hexagonal morphological transition in mixed bilayers may be attributed to an enhanced membrane surface tension that is induced by the vesicle adhesion onto the solid surface. In the next section, we adopt such a model describing the modulation instability in mixed membranes.[10] We then analyze the consequence of this model as surface tension is increased. Some discussion and extensions of our model are provided in section III.

II. Model and Results

The main component of the model is to introduce a coupling between the local composition on the membrane plane and the local curvature. Rather than considering a closed-form vesicle of finite area and enclosed volume, we deal here with a simpler planar and extended membrane. Its shape is then described by the displacement $h(x, y)$ relative to the reference $x-y$ plane. The local relative composition (assuming a simple binary mixture of two components) is denoted by $\phi(x, y)$. The total free energy is written in terms of these two local fields. For simplicity, we consider only small undulations above the $x-y$ plane in the form of a phenomenological expansion proposed in ref 10

$$H\{h, \phi\} = \int d^2x \left[\frac{\sigma}{2}(\nabla h)^2 + \frac{\kappa}{2}(\nabla^2 h)^2 + \frac{b}{2}(\nabla\phi)^2 + \frac{a_2}{2}\phi^2 + \frac{a_4}{4}\phi^4 - \mu\phi + \Lambda(\nabla^2 h)\phi \right] \quad (1)$$

where $\sigma > 0$ and $\kappa > 0$ are the surface tension and bending rigidity of the membrane, respectively. The parameter $b > 0$ is related to the line tension between different domains, and $a_2 \propto T - T_c$ is the reduced temperature (T_c is the critical temperature). Below the phase transition, a_2 is negative, and we need to include in the expansion a positive fourth-order term, $a_4 > 0$, for stability purposes. The coefficient of the linear term, μ, is the chemical potential. Finally, Λ is the composition−curvature coupling constant. This coupling term represents the situation where the spontaneous curvature of the membrane depends on the local composition. For simplicity, other coupling terms such as $(\nabla^4 h)\phi$ (that has a higher gradient order) as well as higher-order coupling terms are omitted.
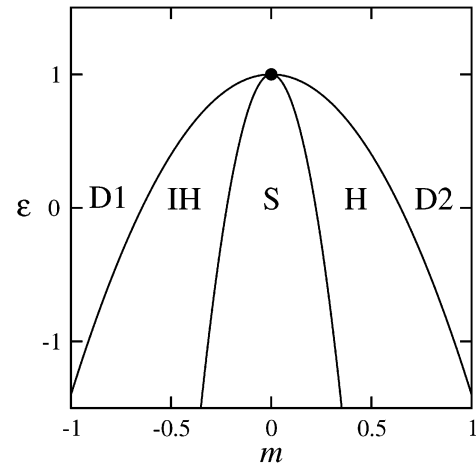
Starting from the above free energy, we first integrate out the h-field in Fourier space. Then the effective free energy is expanded in powers of the gradient of ϕ.[10,11]

$$H_{\text{eff}}\{\phi\} \approx \int d^2x \left[\frac{B}{2}(\nabla\phi)^2 + \frac{C}{2}(\nabla^2\phi)^2 + \frac{a_2}{2}\phi^2 + \frac{a_4}{4}\phi^4 - \mu\phi \right] \quad (2)$$

where

$$B \equiv b - \frac{\Lambda^2}{\sigma} \qquad C \equiv \frac{\Lambda^2\kappa}{\sigma^2} \quad (3)$$

In deriving the above expression, we performed an expansion up to fourth order in the wavevector q (or equivalently up to fourth order in the differential operator in real space). When $B < 0$ (or $\Lambda^2 > b\sigma$), the coefficient of $(\nabla\phi)^2$ becomes negative, leading to an instability of the homogeneous system with respect

(9) Cuvelier, D.; Chiaruttini, N.; Bassereau, P.; Nassoy, P. *Europhys. Lett.* **2005**, *71*, 1015.
(10) Leibler, S.; Andelman, D. *J. Phys. (Paris)* **1987**, *48*, 2013.
(11) Brazovskii, S. A. *Sov. Phys. JETP* **1975**, *41*, 85.

Figure 2. Mean-field phase diagram in the (m, ε) plane. m represents the reduced composition, and ε represents the reduced temperature as defined in eq 6. There are four different phases: the disordered phase (denoted D1 and D2 on the two sides of the transition lines), the striped phase (S), the hexagonal phase (H), and the inverted hexagonal phase (IH). These phases are separated by first-order transition lines. For simplicity, we show here by solid lines only the crossover in the free energies while avoiding plotting two-phase regions. The filled circle located at $(m, \varepsilon) = (0, 1)$ indicates the critical point. Reproduced from ref 10.

to long-wavelength fluctuations. In this case, the magnitude of the most unstable wavevector is given by $q^* = (-B/2C)^{1/2}$. Notice that the sign of Λ can also be negative because B and C depend only on Λ^2.

The phase diagram can be constructed by comparing the mean-field free energies of the striped and the hexagonal phases. The stripe order parameter is

$$\phi_S = \phi_0 + \phi_{q^*}\cos(q^*x) \quad (4)$$

where $\phi_0 = \langle\phi\rangle$ is the spatially averaged composition (imposed by the chemical potential μ) and ϕ_{q^*} is the amplitude of the q^*-mode in the x direction. Similarly, the local composition of the hexagonal phase $\phi_H(\vec{r})$ is given by a superposition of three modes:

$$\phi_H = \phi_0 + \sum_{i=1}^{3} \phi_{q^*}\cos(\vec{q}_i\cdot\vec{r}) \quad (5)$$

Here $\vec{q}_1$, $\vec{q}_2$, and $\vec{q}_3$ are arranged symmetrically on a 2D circle such that $|\vec{q}_i| = q^*$ and $\sum_{i=1}^{3}\vec{q}_i = 0$. Only the most unstable wavevector q^* (single-mode approximation) is used in the calculation. This can be justified for the weak segregation region close to the critical point, $T \lesssim T_c$. In Figure 2, we reproduce the original phase diagram of ref 10. It is presented in terms of the reduced temperature and the reduced average composition defined, respectively, by

$$\varepsilon \equiv \frac{4Ca_2}{B^2} \qquad m \equiv \left(\frac{4Ca_4}{B^2}\right)^{1/2}\phi_0 \quad (6)$$

whereas the surface tension σ and other parameters included in B and C are fixed. (We have corrected the numerical prefactors of "2" in eq 10 of ref 10 in the above equations.)

Four distinct phases—disordered (D), striped (S), hexagonal (H), and inverted hexagonal (IH)—can be seen in Figure 2. Regions of coexistence are omitted here for clarity. Thus, the transition lines indicate the locus of points at which the free energies of different phases cross each other. The calculated phase diagram is in qualitative agreement with experiments

performed on mixtures of lipids in Langmuir monolayers at the air−water interface.[12]

To see the role of surface tension clearly, we cannot directly use the above phase diagram of Figure 2 because σ enters into the two reduced variables, ε and m, via prefactors B and C. Instead, we construct a new phase diagram in terms of two different reduced variables defined by

$$\Omega \equiv \frac{a_2}{a_4\phi_0^2} \qquad \Sigma \equiv \frac{b\sigma}{\Lambda^2} \qquad (7)$$

These two variables are related to ε and m by

$$\Omega = \frac{\varepsilon}{m^2} \qquad \Sigma = 1 - \frac{(4\kappa a_4)^{1/2}\phi_0}{\Lambda m} \qquad (8)$$

We note that Ω is independent of the surface tension parameter σ and that the only variation of σ enters into the second variable, $\Sigma \sim \sigma$. With the use of these new variables, the phase diagram can be drawn for a given value of $M \equiv (4\kappa a_4)^{1/2}\phi_0/\Lambda$. Different values of M correspond to different values of the average composition ϕ_0 when the coupling constant Λ, a_4, and the bending modulus κ are kept fixed. Physically, this is quite reasonable because we expect the latter parameters to have only a weak dependence on temperature and composition.

Figure 3 is the calculated phase diagram in the (Ω, Σ) plane for two choices of the parameter M: $M = 0.1$ and 0.2. The reason behind choosing these M values will be discussed later. Because Ω is a function of ϕ_0^2, this phase diagram does not distinguish between the hexagonal (H) and inverted hexagonal (IH) phases or between the disordered condensed (D1) and dilute (D2) phases in Figure 2. (The inverted hexagonal phase and the disordered condensed phase appear when $\phi_0 < 0$.) Generally, the striped phase (S) exists when $\Sigma \sim \sigma$ is small. The dashed arrow in Figure 3 indicates a horizontal path along which Σ (or, equivalently, the surface tension σ) increases for a fixed value of Ω. Clearly, along this path the striped phase (S) transforms into the hexagonal phase (H) via a first-order phase transition. As Σ increases even further, there will be another first-order phase transition into the homogeneous disordered phase (D).

It should be noted that although the calculated phase diagram depends on the value of M the sequence of the modulated structures remains unchanged. Such a sequence of pattern transformation, S → H, upon increasing the surface tension is consistent with the sequence observed in the mixed lipid bilayers.[6] Hence, we consider that the enhanced surface tension during the adhesion process is responsible for the morphological evolution of the domain shapes in the adhering vesicle. This is the main claim of the present paper. In the experiment of ref 6, they observed that the area of the vesicle increased in time. This may be due to the enhanced surface tension which acts to pull and expand the vesicle. Moreover, the experiment shows that the ordered hexagonal lattice further evolved to disordered circular domains with elapsed time. Such a situation may correspond to a transient state when the membrane undergoes a transition from the hexagonal phase (H) to the disordered phase (D) as the surface tension increases.

To make a comparison with ref 6, we give here the estimated values for the model parameters in eq 1. The surface tension of an adhering vesicle can be in the range of 5×10^{-6} to 10^{-4} J/m^2, and we have chosen here $\sigma \simeq 10^{-5}$ J/m^2.[13] The other parameters can be found in refs 7 and 14 as $\kappa \simeq 25k_BT \simeq 10^{-19}$ J and $b \simeq$
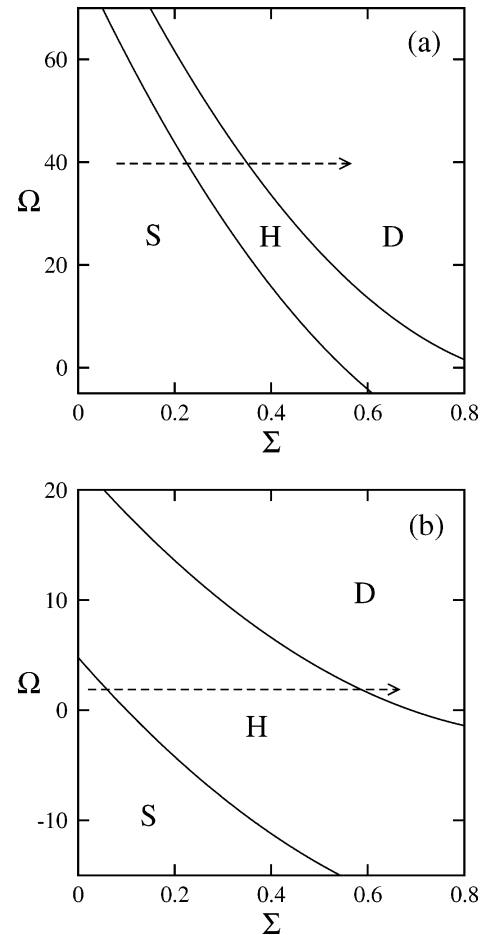
Figure 3. Mean-field phase diagram in the (Σ, Ω) plane for (a) $M = 0.1$ and (b) $M = 0.2$. Σ represents the reduced surface tension, and Ω represents the temperature−composition coupling parameter, as defined in eq 7. The definitions of the different phases are the same as in Figure 2. The effect of increasing the surface tension is represented by the dashed right-hand arrow.

$5\kappa \simeq 5 \times 10^{-19}$ J. Although there is no direct measure of the coupling constant value, Λ can be estimated by fitting the experimentally observed modulation period (roughly 1×10^{-6} m for the striped phase) with $2\pi/q^*$. Then we obtain the coupling constant as $\Lambda \simeq 4.9 \times 10^{-12}$ J/m. This estimation is consistent with that mentioned in ref 14. Using these values, the surface tension required to induce the striped-to-hexagonal transition can be evaluated as $\sigma \simeq \Sigma \times (4.7 \times 10^{-5})$ J/m^2. For instance, $\sigma = 1.4 \times 10^{-5}$ J/m^2 when $\Sigma = 0.3$. Along the dashed right-hand arrows in Figure 3, the most unstable mode changes as $q^* \sim [\Sigma(1 - \Sigma)]^{1/2}$.

Furthermore, if we assume a_4 to be of the same order as σ and set $a_4 \simeq 10^{-5}$ J/m^2, then the parameter values $M = 0.1$ and 0.2 are equivalent to setting $\phi_0 = 0.24$ and 0.48, respectively. These values are physically relevant and represent asymmetric binary mixtures. Naturally, the modulation instability does not occur if the model parameters do not satisfy the necessary condition $B = b - \Lambda^2/\sigma < 0$, but with our above choice of parameters, we are in the instability regime $B < 0$.

III. Discussion

We have studied the effect of surface tension on a curvature instability that is coupled to a lateral phase separation. Although

(12) Keller, S. L.; McConnell, H. M. *Phys. Rev. Lett.* **1999**, *82*, 1602.
(13) Hu, J.-G.; Granek, R. *J. Phys. II* **1996**, *6*, 999.

(14) Rädler, J.; Feder, T.; Strey, H.; Sackmann, E. *Phys. Rev. E* **1995**, *51*, 4526.

eq 1 provides a minimum and sufficient model to see such an effect, several points merit further discussion.

(i) We have considered only an average flat and extensive membrane rather than closed-shaped vesicles of finite area and volume. In the case of closed-shaped vesicles, the principle mechanism of the tension-induced transition should prevail, but a pressure difference across the vesicle should be taken into account because it plays an important role in the selection of the most stable modes on the vesicle.[15−17]

(ii) The present model is valid for membranes composed of a binary mixture, although a ternary mixture is used in ref 6. Nevertheless, the local composition ϕ can be taken as the composition of one of the lipids, say sphingomyelin or DOPC, with respect to its critical value. This is because the liquid-ordered phase may be only moderately enriched in cholesterol. An extension of the present model to a ternary mixture is also possible following ideas similar to those in ref 18.

(iii) As stated before, we considered the weak segregation limit of the lateral phase separation, which is valid when the two phases are only weakly immiscible. Such an approximation was taken in refs 10 and 17, whereas the opposite strong-segregation limit was investigated in refs 15, 16, 19, and 20. At present, it is not clear which approximation is more appropriate to account for the experimentally observed patterns because the experimental system probably lies in an intermediate regime. In a recent paper dealing with the strong segregation limit,[20] however, the striped phase exists between the hexagonal and the disordered phases, and the increased surface tension causes a *reverse* transition from the hexagonal to the striped phase. Although the experimentally observed sequence of the transition is in qualitative agreement with the trend found in our weak segregation theory, more work needs to be done before further conclusions can be drawn. In particular, there is a need to do experiments where the surface tension is either controlled or measured directly. That will allow a more quantitative agreement between theory and experiment.

(iv) In other generalizations of the model, the bilayer nature of the membrane can be taken into account explicitly. In the case of mixed vesicles, the spontaneous curvature arises from the asymmetry in the composition between the inner and outer leaflets comprising the bilayer membrane.[21,22] Asymmetry in the composition occurs in situations where the two leaflets experience a different environment as well as in biological cells because of active (in vivo) processes.[23] Although the evidence of the asymmetric composition between the inner and outer leaflets has not been reported in ref 6, it might exist for an adhering mixed vesicle because only the outer leaflet is in contact with the surface. More detailed theories dealing with the bilayer nature of the membranes are given in refs 18 and 24 and can be generalized to the present case of mixed vesicles.

We next discuss how the present work is related to previous models beside refs 19−20. Hu and Granek[14] investigated the buckling of mixed amphiphilic monolayers by considering similar coupling between the composition and the curvature. In their work, the surface tension is introduced as a Lagrange multiplier in order to ensure the fixed total area of the monolayer (fixed area ensemble). In our case, however, the surface tension is regarded as a control parameter of the membrane shape (fixed surface tension ensemble). Despite the difference in the working ensembles, they also predicted that a transition from the striped to the hexagonal phases can be induced either by decreasing the coupling constant (Λ in our paper) and/or increasing the line tension b (Figure 3 in ref 14). Notice that both parameter changes are equivalent to increasing Σ, as seen in eq 7, and our result is consistent with theirs.

In previous experiments of ref 4, similar striped and hexagonal patterns have been shown, but no similar temporal evolution was reported. This may be because the vesicles in ref 4 were suspended in an aqueous solution (rather than adhering onto a surface) and their surface tension is not increasing as function of time. It is also not entirely clear how much the patterns and domains seen on the vesicular surface are truly equilibrium ones or just long-lived metastable ones.

Finally, we comment on the dynamical aspect of the observed morphological transition. In the past decade, kinetics of phase transitions between different ordered mesophases have been studied intensively, especially for block copolymer systems.[25] Among various works, Nonomura and Ohta investigated the morphological transition between the lamellar and the hexagonal phases in two dimensions.[26] Their dynamical equation is based on the time-dependent Ginzburg−Landau equation using a free energy that includes a long-range repulsive interaction term. This free energy is known to be similar to the one used in the present work.

In ref 26, the transition is induced by changing the temperature. Note that in our Figure 3 a change in temperature is simply a vertical scan where $\Omega \sim a_2 \propto T - T_c$ changes, whereas $\Sigma \sim \sigma$, M, and ϕ_0 are kept fixed. The vertical scan can also lead to a crossover between the striped and hexagonal phases. In the experiments,[6] however, the temperature is kept fixed, and we consider that the origin of the transition relies on the temporal increase in the surface tension as detailed above. Despite the difference in the control parameters (either temperature or surface tension), the time evolution of the structure in the simulation[26] is very similar to that observed for the lipid mixtures. For example, the stripes undergo a pearling phenomenon, and the hexagonal domains appear at the grain boundaries of the lamellar structure. We hope that more quantitative measurements of the surface tension during the adhesion process will shed light on this intriguing phenomena and will lead to further theoretical investigations.

(15) Andelman, D.; Kawakatsu, T.; Kawasaki, K. *Europhys. Lett.* **1992**, *19*, 57.
(16) Kawakatsu, T.; Andelman, D.; Kawasaki, K.; Taniguchi, T. *J. Phys. II* **1993**, *3*, 971.
(17) Taniguchi, T.; Kawasaki, K.; Andelman, D.; Kawakatsu, T. *J. Phys. II* **1994**, *4*, 1333.
(18) Kumar, P. B. S.; Gompper, G.; Lipowsky, R. *Phys. Rev. E* **1999**, *60*, 4610.
(19) Harden, J. L.; MacKintosh, F. C. *Europhys. Lett.* **1994**, *28*, 495.
(20) Harden, J. L.; MacKintosh, F. C.; Olmsted, P. D. *Phys. Rev. E* **2005**, *72*, 011903.
(21) Safran, S. A.; Pincus, P. A.; Andelman, D.; MacKintosh, F. C. *Phys. Rev. A* **1991**, *43*, 1071.
(22) MacKintosh, F. C.; Safran, S. A. *Phys. Rev. E* **1993**, *47*, 1180.
(23) Keller, S. L.; Pitcher, W. H.; Huestis, W. H., III; McConnell, H. M. *Phys. Rev. Lett.* **1998**, *81*, 5019.
(24) Kodama, H.; Komura, S. *J. Phys. II* **1993**, *3*, 1305.
(25) Qi, S.; Wang, Z.-G. *Phys. Rev. Lett.* **1996**, *76*, 1679. Qi, S.; Wang, Z.-G. *Phys. Rev. E* **1997**, *55*, 1682.
(26) Nonomura, M.; Ohta, T. *J. Phys. Soc. Jpn.* **2001**, *70*, 927.